observed, without cluster formation.

Acknowledgment. This work was partly supported by the Natural Sciences and Engineering Research Council of Canada (NSERC).

References

1. Eisenberg, A.; King, M. *Ion-Containing Polymer, Physical Properties and Structure*; Academic Press: New York, U. S. A., 1977.
2. Eisenberg, A. *Macromolecules* **1970**, *3*, 147.
3. Wilson, F. C.; Longworth, R.; Vaughan, D. J. *Polym. Prepr. (Am. Chem. Soc., Div. Polym. Chem.)* **1968**, *9*, 505.
4. Eisenberg, A.; Hird, B.; Moore, R. B. *Macromolecules* **1990**, *23*, 4098.
5. Hird, B.; Eisenberg, A. *J. Polym. Sci., Part B: Polym. Phys.* **1990**, *28*, 1665.
6. Kim, J.-S.; Jackman, R. J.; Eisenberg, A. *Macromolecules* **1994**, *27*, 6541.
7. Ma, X.; Sauer, J. A.; Hara, M. *Macromolecules* **1995**, *28*, 3953.
8. Ma, X.; Sauer, J. A.; Hara, M. *Polymer* **1997**, *38*, 4425.
9. Gronowski, A. A.; Jiang, M.; Yeager, H. L.; Wu, G.; Eisenberg, A. *J. Membr. Sci.* **1993**, *82*, 83.
10. Jiang, M.; Gronowski, A. A.; Yeager, H. L.; Wu, G.; Kim, J.-S.; Eisenberg, A. *Macromolecules* **1994**, *27*, 6541.
11. Tong, X.; Bazuin, C. G. *J. Polym. Sci.: Part B: Polym. Phys.* **1992**, *20*, 389.
12. Wollmann, D.; Williams, C. E.; Eisenberg, A. *Macromolecules* **1992**, *25*, 6775.

Electronic Band Structure of N and P Dopants in Diamond

Dae-Bok Kang

Department of Chemistry, Kyungsung University, Pusan 608-736, Korea
Received January 11, 1998

The properties of the n-type impurities nitrogen and phosphorus in diamond have been investigated by means of electronic band structure calculations within the framework of the semiempirical extended Hückel tight-binding method. For diamond with the nitrogen and phosphorus substitutional impurities, calculated density of states shows the impurity level deep in the band gap. This property can be derived from the substantial <111> relaxation of the impurity and nearest-neighbor carbon atoms, which is associated with the population of an antibonding orbital between them. The passivated donor property of the P-vacancy complex which lies deep in the gap is also discussed.

Introduction

Recent advances in diamond-film growth techniques have stimulated an interest in the use of diamond as a semiconductor in electronic devices.[1] Diamond films produced by low-pressure methods have a wide array of potential applications due to their unique mechanical, thermal, optical, and semiconducting properties. Despite the significant process in the field of diamond growth, the problem of reproducible doping by donor and acceptor impurities to obtain p-n junction remains unresolved. It is well known that p-type conductivity can be obtained by boron doping. The results reported so far on n-type doping are controversial.[2] There is continuing interest in making shallow n-type diamond to develop the p-n technologies of the semiconductor industry applicable to future diamond-based devices. Nearly all of the n-type diamond which has been reported to result from either doping during film growth or ion implantation is highly resistive. An understanding of the behavior of impurities in diamond is important as a tool in the search for a possible n-type dopant.

Substitutional nitrogen and phosphorus with five valence electrons are prototype n-type impurities in diamond. While the isolated nitrogen impurity is well characterized experimentally,[3-8] the phosphorus doping has not been widely reproduced.[9,10] The problem of nitrogen and phosphorus impurities in diamond has also been addressed using a number of theoretical techniques.[11-16] Nonetheless, a complete quantitative description of the impurity energetics and structure is still lacking. Self-consistent molecular orbital calculations by Astier *et al.* predicted a deep donor level occurring at 1.3 eV below the diamond conduction band edge for the substitutional nitrogen impurity.[11] This level was degenerate and therefore assumed to be Jahn-Teller unstable with respect to a distortion. However, self-consistent Green's function calculations on this impurity in diamond find a non-degenerate shallow level (0.15 eV below the conduction band edge) and therefore no Jahn-Teller instability.[12] The authors suggest that the off-center distortion of nitrogen is driven by local bonding effects. Theoretical calculations[13] based on the local-density approximation show that phosphorus is a deep donor at 1.09 eV below the bottom of the conduction band; however, calculations[14,15] using the plane-wave pseudopotential method predict that phosphorus would

take a single atomic substitutional site and be a shallow donor with a level at 0.2 eV. This makes phosphorus potentially interesting as a substitutional n-type dopant in diamond, but it will be very difficult to incorporate it because of its large atomic size. In the semiempirical molecular orbital study by Anderson and Mehandru[16] it was calculated to bind in a diamond monovacancy site about 10 eV more weakly than a carbon atom, whereas a nitrogen atom was calculated to bind only 4 eV more weakly than the carbon atom. This instability of phosphorus in diamond is in part caused by a promoted electron occupying the P-C antibonding orbital. This antibonding orbital is pushed high above the top of the gap region because the large size of the P 3p orbitals overlaps the 2p orbitals of the neighboring carbon atoms strongly, dumping its electron at the bottom of the conduction band.

In spite of a considerable amount of work carried out on incorporating phosphorus in diamond with the aim of making a shallow donor defect, almost all chemical vapor deposition (CVD) grown diamond still remains highly resistive.[17-20] The absence of n-type conduction in this CVD diamond could be attributed either to the nitrogen contamination which compensates substitutional phosphorus or to the formaton of phosphorus-vacancy complexes. Positron annihilation studies[21] show that vacancies are common defects in CVD diamond. The lack of an optical signal due to vacancies in the P-rich material suggests that they are bound up with P in some form. In this paper we study the electronic properties of N and P atoms in substitutional monovacancy sites, P-N disubstitutional pairs, and phosphorus-vacancy complexes using the extended Hückel tight-binding (EHTB) method.[22-24] In particular, we concentrate on a better understanding of the bonding relations of these impurities in diamond. Since first-principles quantum-mechanical cluster calculations are presently limited by available computing resources to two or three shells of carbon atoms, we avoid the problem of surface reconstruction, passivation, and dangling bond states which otherwise would interfere with the states of the substitutional defect in the gap by using the supercell framework and periodic boundary conditions of the semiempirical EHTB method.

Calculational method

The band structure calculations of the diamond impurity system were carried out in the crystalline extension of the extended Hückel method. For each Slater-type atomic orbital (AO) ϕ_ν, a corresponding Bloch sum $b_\nu(\boldsymbol{k})$ is given as

$$b_\nu(\boldsymbol{k}) = 1/N \sum_{p=1}^{N} \exp(i\boldsymbol{k}\cdot\boldsymbol{R}_p)\,\phi_\nu(\boldsymbol{r}-\boldsymbol{R}_p), \tag{1}$$

where the sum is made over the N cells in the solid and $\boldsymbol{k}$ is the wave vector of the Bloch state. The crystal orbital $\psi_i(\boldsymbol{k})$ are expanded as linear combinations of the basis Bloch sums,

$$\psi_i(\boldsymbol{k}) = \sum_{\nu=1}^{n} C_{i\nu}(\boldsymbol{k})\, b_\nu(\boldsymbol{k}), \tag{2}$$

where n is the number of Bloch functions (*i.e.*, the number of AO's in the cells) in the basis set. For each $\psi_i(\boldsymbol{k})$, the eigen energies $e_i(\boldsymbol{k})$ and the coefficients $C_{i\nu}(\mathbf{k})$ are obtained from the solutions of the determinantal equation and the secular equation:

$$|\,\boldsymbol{H}(\boldsymbol{k}) - \boldsymbol{S}(\boldsymbol{k})e_i(\boldsymbol{k})\,| = 0 \tag{3}$$

$$(\boldsymbol{H}(\boldsymbol{k}) - \boldsymbol{S}(\boldsymbol{k})e_i(\boldsymbol{k}))\boldsymbol{C}(\boldsymbol{k}) = 0 \text{ for } i = 1 \text{ to } n. \tag{4}$$

Here, $\boldsymbol{C}(\boldsymbol{k})$ is the matrix of coefficients, the elements of which are the $C_{i\nu}$ $(\mathbf{k})$'s. $\boldsymbol{H}(\boldsymbol{k})$ and $\boldsymbol{S}(\boldsymbol{k})$ are the Hamiltonian and overlap matrices, respectively, and their elements are defined by

$$H_{\mu\nu}(\boldsymbol{k}) = \langle b_\mu(\boldsymbol{k}) \,|\, H^{eff} \,|\, b_\nu(\boldsymbol{k})\rangle \tag{5}$$

$$\text{and } S_{\mu\nu}(\boldsymbol{k}) = \langle b_\mu(\boldsymbol{k}) \,|\, b_\nu(\boldsymbol{k})\rangle. \tag{6}$$

The expansion of $S_{\mu\nu}(\boldsymbol{k})$ contains overlap integrals $\langle\phi_\mu(\boldsymbol{r}-\boldsymbol{R}_p)|\phi_\nu(\boldsymbol{r}-\boldsymbol{R}_q)\rangle$ which are in practice neglected when $|\boldsymbol{R}_p - \boldsymbol{R}_q| > 10$ Å. Similarly, the $H_{\mu\nu}(\mathbf{k})$ expands on $\langle\phi_\mu|H^{eff}|\phi_\nu\rangle$ terms. The atomic parameters used in these calculations are the Slater exponents ζ of the Slater orbitals and the diagonal elements of the effective Hamiltonian H^{eff}, $\langle\phi_\mu|H^{eff}|\phi_\mu\rangle$. These parameters are given in Table 1. The off-diagonal elements of the Hamiltonian are calculated by means of the modified Wolfsberg-Helmholz approximation.[26] The band structure calculations used a 24-atom supercell shown in Figure 1. The C-C bond distance is set at 1.54 Å except when there is an inclusion of impurity-atom relaxation in the diamond lattice. A 64 k-point mesh of the irreducible part of the Brillouin zone was used to compute the density of states (DOS) and the crystal orbital overlap populations (COOP) for the 3D solid.

Table 1. Atomic parameters used in the calculations.[38] Slater orbital exponents ζ (a.u.) and diagonal Hamiltonian matrix elements H^{eff} (eV)

atom	orbital	H^{eff}	ζ
C	2s	−21.4	1.625
	2p	−11.4	1.625
N	2s	−26.0	1.950
	2p	−13.4	1.950
P	3s	−18.6	1.75
	3p	−14.0	1.30

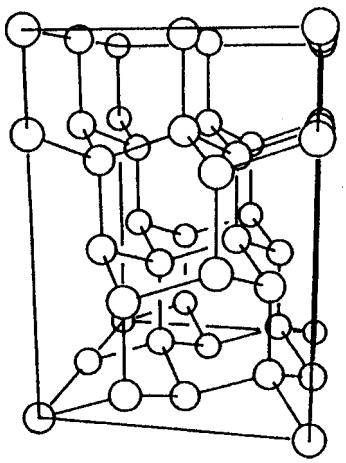

Figure 1. Unit cell of the diamond lattice used for defect studies.

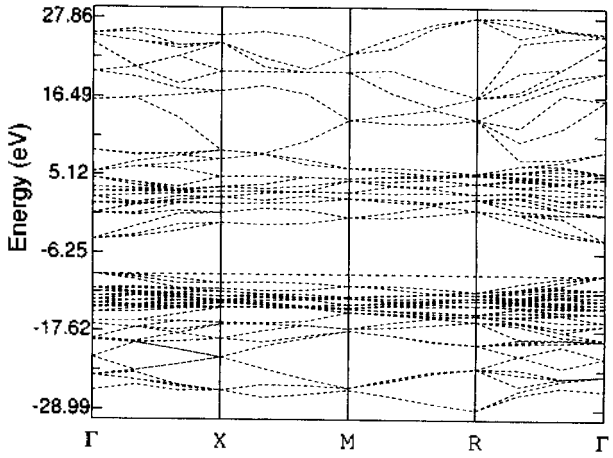

Figure 2. EHTB band structure of diamond. The horizontal dashed line indicates the Fermi level.

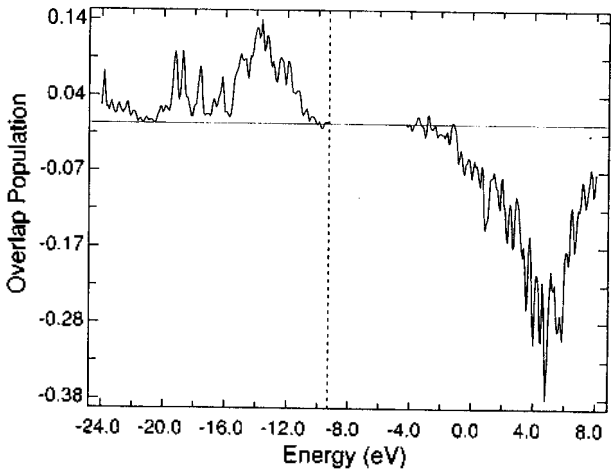

Figure 4. COOP curves for the C-C bond. The vertical dashed line indicates the Fermi level.

Results and discussion

Pure diamond in absence of defect. The band structure of the perfect diamond crystal is shown in Figure 2. All symmetry lines of the orthorhombic Brillouin zone were considered in the calculations. The valence band structure exhibits rather flat energy bands with little variation in energy along the symmetry direction. The conduction band structure shows somewhat greater curvature than that of the valence band. There is a band gap of 5.0 eV which separates the valence from the conduction bands, while the observed gap is 5.5 eV.[37] The unit cell of C_{24} contains 96 valence electrons. There are 48 valence bands in C_{24} and each band is occupied by two electrons; hence, the valence bands can be completely filled and the diamond is expected to be an insulator.

The total and projected density of states for the perfect diamond are shown in Figure 3. The low-energy end of the valence band energy spectrum (−33.2 to −22.2 eV) is dominated by the C 2s atomic states. This is followed by a region 2.5 eV wide in which the states consist of carbon 2s and 2p orbitals. Finally, the high-energy section of the valence band contains pure carbon 2p states. For the conduction band, there is a significant contribution from the C 2p states in the low-lying energy areas of the band structure. Both band-edge states are dominated by the C 2p orbitals and these are strongly split by the effect of bonding and antibonding interactions between the 2p orbitals of the neighboring C atoms.

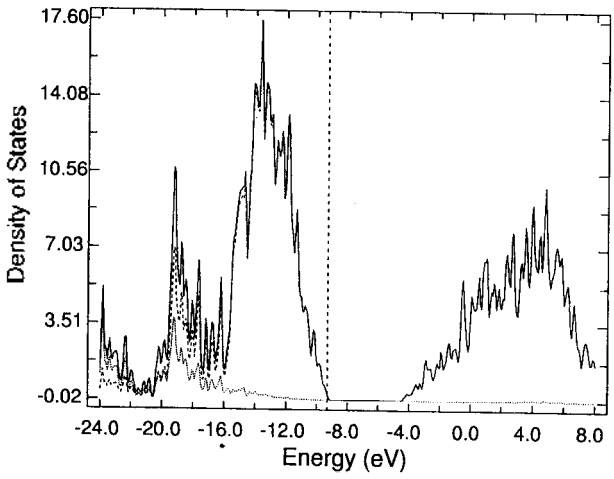

Figure 3. Partial DOS of C in diamond (... 2s contribution, --- 2p contribution). The vertical dashed line indicates the Fermi level.

In order to understand the nature of the chemical bonding in diamond we need to look at the COOP[27] for a given bond. Essentially, these curves tell us the bonding, nonbonding or antibonding nature of the levels in a certain energy range. Those for the C-C bond are shown in Figure 4. Below the gap at −9.3 eV, all the filled states are bonding, but above the gap strong antibonding features develop. An electron count above the electron filling of 96 electrons would have a destabilizing effect.

Substitutional N. Substitutional nitrogen, with five valence electrons, is expected to be an n-type impurity in diamond. However, nitrogen impurity is accepted to introduce a deep level 1.7-2.1 eV below the bottom of the conduction band.[7,8] There have been several theoretical investigations into nitrogen in diamond.[11~14,28~32] The focus of these calculations has been on the length of the single long C-N internuclear distance, which is reported as the percent increase over the bulk diamond nearest-neighbor distance of 1.54 Å. The atoms neighboring N were relaxed giving rise to a trigonal distortion. In the present work, we do not address the problem of the position of an impurity atom in the diamond lattice, but rather focus on the effect of the relaxed structure around the N atom on the electronic properties of N-doped diamond. For nitrogen occupying a relaxed substitutional site, the distortion is assumed to occur in the <111> direction with N atom and the <111> C atom moving away from the N so that the defect has the same local structure as determined in Ref. 25. Figure 5 shows a schematic model of the orbital correlation diagram associated with the bonding of the substitutional N atom to the vacancy site in diamond. The dangling orbitals due to the carbon vacancy are located near the top of the valence band. The nitrogen impurity produces two states of interest,

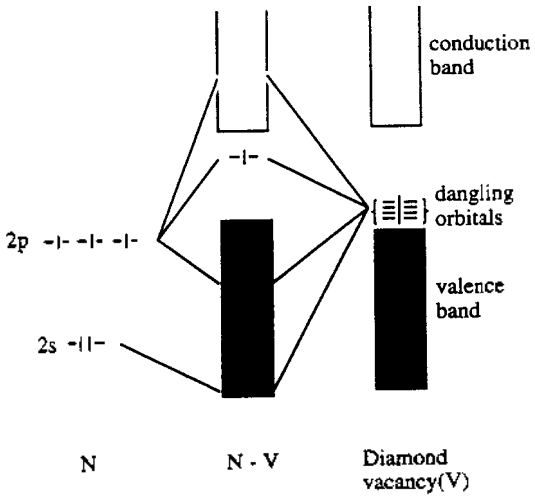

Figure 5. Schematic orbital correlation diagram of the levels induced by the N atom binding to a carbon vacancy in diamond.

the bonding and antibonding combinations of the N 2s and 2p orbitals mixed with the C dangling-bond orbitals, essentially localized on the four carbon atoms surrounding the vacancy. All bonding orbitals formed from the overlap of the N atomic orbitals with the dangling orbitals lie in the valence band as shown in Figure 5. Note that a singly occupied orbital in the gap is the antibonding combination of the N and C 2p orbitals along the <111> direction. In the absence of lattice relaxation the singly occupied C-N σ^* orbital is located at the bottom of the conduction band. This system is expected to be unstable toward structural distortions to stabilize the antibonding state singly occupied. A single C-N bond stretch along the <111> direction allows the C-N σ^* orbital to lower into the mid-band gap in energy. It is the antibonding occupancy which is the source of a distortion which moves the carbon and the nitrogen atoms from each other. The C-N bond distance increased by 0.46 Å from the diamond value of 1.54 Å reflects its bond order of 1/2. Its Mulliken overlap population is calculated to be 6.

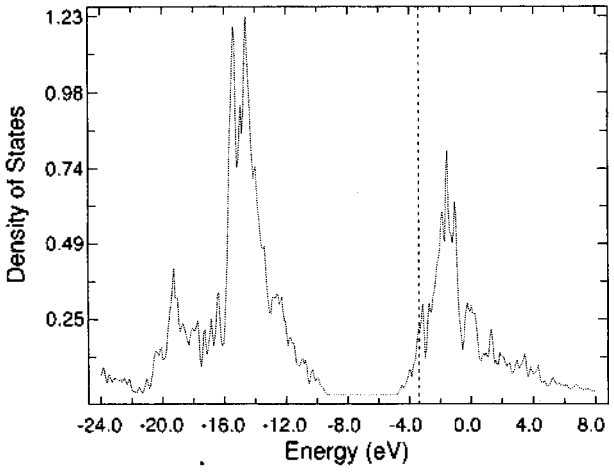

Figure 6. Partial DOS of single substitutional nitrogen in "unrelaxed" diamond. The vertical dashed line indicates the Fermi level.

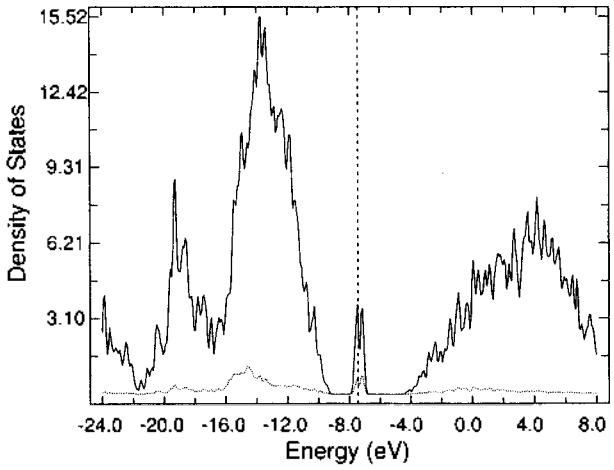

Figure 7. Partial DOS of single substitutional nitrogen in "relaxed" diamond with the relaxation of N and C along <111> only. The solid line represents the total DOS. The vertical dashed line indicates the Fermi level.

7% that of the other three C-N single bonds. The DOS curve for the 24-atom supercell with the central C atom replaced with N is shown in Figure 6, in which the gap state appears as a shoulder on the low-energy side of the diamond conduction band. Figure 7 shows the projected DOS curve of the impurity donor state which appears in the band gap when the geometrical relaxation of the nitrogen impurity stated above is considered. This result can be explained by remarking that the N donor state bands lying rather deep in the gap are in nature antibonding, so that they are derived almost exclusively from the conduction band states. The COOP curve in Figure 8 confirms this. These calculated donor bands are too deep to lead to appreciable conductivity, consistent with observed behavior.[7,8]

Substitutional P. Isovalent with nitrogen, phosphorus is predicted to be a shallow donor.[14,16] This is because its orbital overlap with neighboring C atoms is much larger compared to that of N so that the half-filled σ^* orbital will be very destabilized, even in the relaxed structure. Theoretical

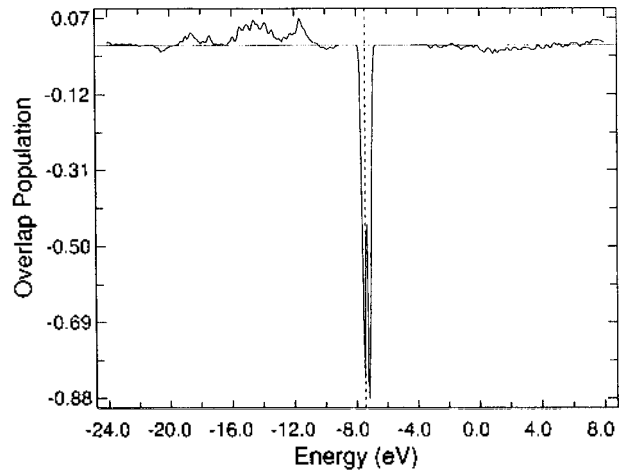

Figure 8. COOP curves for an elongated C-N bond. The vertical dashed line indicates the Fermi level.

studies by Bernholc *et al.*[14] using the plane wave pseudopotential method found that the phosphorus impurity atom remained on-site and the impurity donor level lay 0.2 eV below the bottom of the conduction band. However, the equilibrium solubility of phosphorus in diamond was predicted to be very low, even at the high temperatures. In contrast, a self-consistent local density approximation cluster calculations[13] determined the deep donor level position of 1.09 eV relative to the conduction band edge.

We investigated the electronic properties of this defect by assuming the outward radial relaxation of nearest-neighbors from the impurity atom, holding the remaining atoms in the supercell fixed at their ideal lattice positions. Substitutional phosphorus is to be distinguished from substitutional nitrogen with off-site defect. Both N and one of the C neighbors in the latter move off-site along <111>, resulting in a substantial bond extention. However, the lattice relaxation around the P impurity in the former is reported to be small.[16] According to the cluster molecular orbital study by Anderson and Mehandru,[16] three P-C bond distances were increased by 0.06 Å and the fourth by 0.08 Å. These P-C bond distances are considerably less than the sum of te of the restoring force of the lattice preventing further separation. For the relaxation of the local C atoms around the impurity site, the trigonal structure given in Ref. 16 was used for the calculations.

In contrast with the N impurity, the donor impurity state is not visible in the band gap as shown in Figure 9. The P impurity state situates high up in the conduction band, which is caused by the strong antibonding nature of the bonds between the phosphorus and the neighboring C atoms, reflecting the large size of the P atomic orbitals. Thus, substitutional P, with a singly occupied level close to the bottom of the conduction band, is predicted to be a shallow donor. However, the experimental results on phosphorus doping are contradictory.[19] Two possible explanations may exist for obtaining a deep donor level due to phosphorus doping. One is that phosphorus is present as P^+, being compensated by deep level traps. In this regard, a recent interesting experimental paper[33] has reported the absence of conductivity for the epitaxial diamond films prepared by the hot-filament CVD technique using phosphine and nitrogen simultaneously as doping sources. We provide an electronic structure explanation for the lack of donor ability of substitutional P codoped with nitrogen using the model of substitutional N-P dimer pairs in the following section. The other is that phosphorus does not enter in singly substitutional form but makes impurity-vacancy complexes. The formation of a phosphorus-vacancy complex in order to accommodate the large phosphorus atom may be preferable comparing with the substitutional position of phosphorus in the diamond lattice. The electronic properties of this complex in diamond are discussed later.

Substitutional P-N dimer pairs. From theoretical calculations[14-16] and experiments,[17-20] it is clear that it would be very difficult to obtain the substitutionally incorporated P in diamond, and this is mainly because of its large size as discussed earlier. Recent experimental works on the P incorporation into the epitaxial films have shown that it could be greatly enhanced by introducing nitrogen simultaneously.[33-35] They found no electrical conductivity. Our EHTB band calculations on the substitutional P-N dimer in diamond lattice are based on the minimum energy structures, including relaxations of the nitrogen and phosphorus atoms and the first carbon shell, which can be found in Ref. 36. One of the N-C bonds stretches to 2.0 Å, having zero bond order. Figure 10 and 11 show the DOS and COOP curves of the doubly occupied N-C σ^* band lying deep in the gap, respectively. P character is not found in the gap. Essentially, this implies that these dimers are polarized as N^--P^+ because of compensation. The reduction of N to N^- with two band gap electrons gives a longer N-C bond with the occupied σ^* state of an energy even deeper in the gap. Being doubly occupied, the N-C gap state drops deep into the gap with its long bond stretch. Consequently, substitutional P-N dimers are calculated to be a deep donor, which accounts for the absence of electrical conductivity and luminescence observed in Ref. 33.

P-vacancy complex. In the calculations for the P-V complex we used trigonal symmetry from which two C atoms were removed and a P atom added. The P atom lies

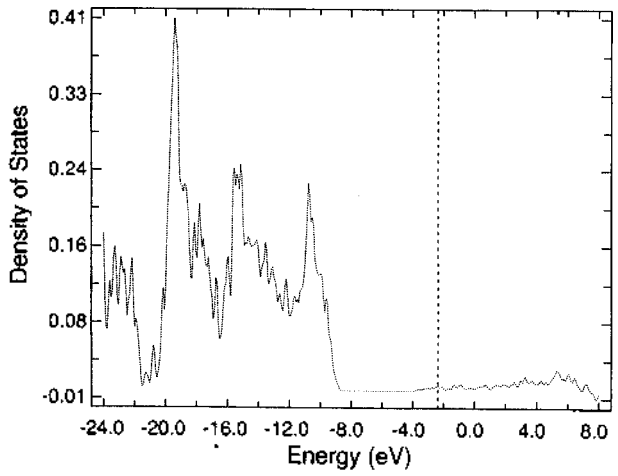

Figure 9. Partial DOS of single substitutional phosphorus in diamond. The vertical dashed line indicates the Fermi level.

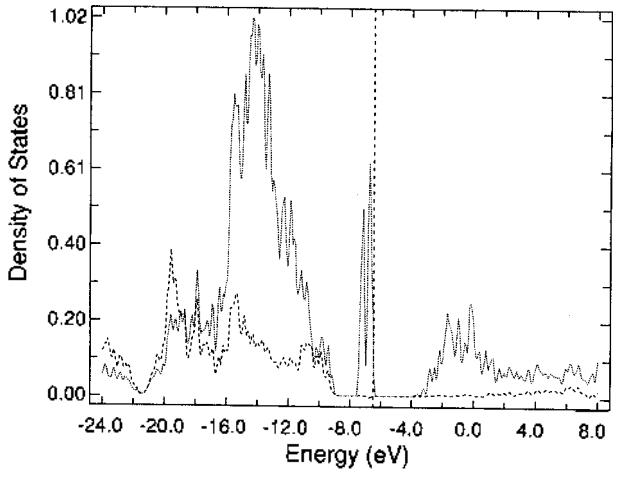

Figure 10. Partial DOS for the N (dotted line) and the P (dashed line) atoms of the substitutional P-N dimer in diamond. The vertical dashed line indicates the Fermi level.

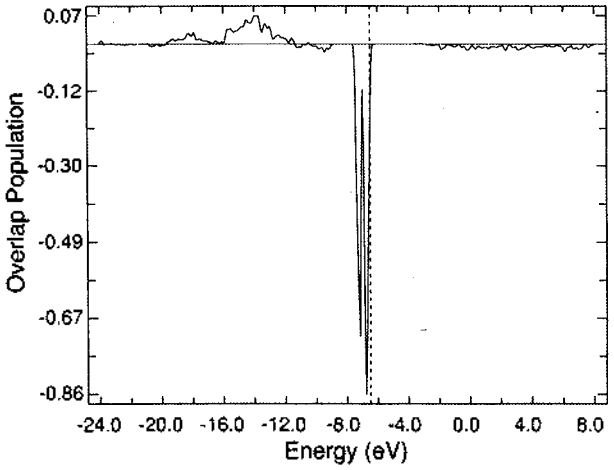

Figure 11. COOP curves for an elongated C-N bond. The vertical dashed line indicates the Fermi level.

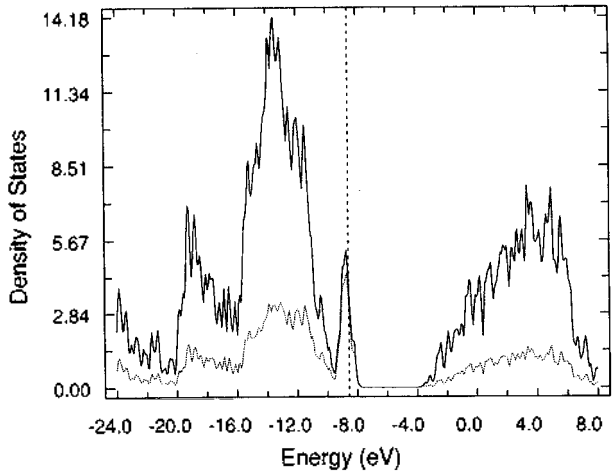

Figure 12. Partial DOS for the six carbon atoms surrounding P of the P-V complex in diamond. The solid line represents the total DOS. The vertical dashed line indicates the Fermi level.

at the midpoint between two neighboring vacancies to generate a P-V pair. The six P-C bond lengths are 1.94 Å. The stability of this split vacancy geometry is partially connected with the large atomic size of P. Figure 12 shows the six dangling bonds of the P-V defect in the region of the band gap. These form a midgap state just above the top of the valence band which is localized on the six C atoms surrounding P and has very little amplitude on P. The position of this midgap state is so deep that the defect would be expected to trap electrons from any donor and act as a deep acceptor. This would be an explanation of considerable difficulty in making phosphorus electrically active in diamond.

Conclusions

We examined the properties of N and P atoms in monovacancy substitutional sites and P-N pairs and P-V complex in divacancy sites. When N donor impurity atom with five valence electrons is introduced in a vacancy in diamond, an electron is promoted to an antibonding orbital of the bond between the donor atom and a neighboring carbon atom. This antibonding occupancy gives an elongation of that bond which brings the N-C σ^* orbital deep into the band gap and accounts for the <111> trigonal distortion observed. By contrast, for the substitutional phosphorus defect P-C σ^* antibonding component can no longer place the level in the band gap to rise above the top of the gap region. It will dump its electron at the bottom of the conduction band. This destabilization is caused by the strong antibonding interactions between the large P atom and the neighboring C atoms, even in the relaxed structure. Despite substitutional P being expected to behave as a donor there is no experimental evidence proving that P-doped diamond shows measurable electrical conductivity or P induced luminescence. This can be explained by the formation of P-N disubstitutional pairs and P-V complex in diamond which are deep donors and compensate substitutional P.

Acknowledgment. This work was supported by the Korea Research Foundation. Discussions with Professor Alfred Anderson are acknowledged.

References

1. (a) Angus, J. C.; Hayman, C. C. *Science* **1988**, *241*, 913. (b) Angus, J. C.; Buck, F. A.; Sunkara, M.; Groth, T. F.; Hayman, C. C.; Gat, R. *Mater. Res. Soc. Bull.* **1989**, *14*, 38.
2. Popovici, G.; Prelas, M. A. In *Diamond-Film Semiconductors*; Tamor, M.; Aslam, M. (eds.), SPIE v. 2151, **1994**, p 99.
3. Walker, J. *Rep. Prog. Phys.* **1979**, *42*, 108.
4. Davies, G. *Rep. Prog. Phys.* **1981**, *44*, 787.
5. Loubser, J.; van Wyk, J. A. *Rep. Prog. Phys.* **1978**, *41*, 1201.
6. Ammerlaan, C. A. J.; Burgemeister, E. A. *Phys. Rev. Lett.* **1981**, *47*, 954.
7. Farrer, R. G. *Solid State Commun.* **1969**, *7*, 685.
8. van Enckevort, W. J. P.; Versteegen, E. H. *J. Phys. Condens. Matter* **1992**, *4*, 2361.
9. Okano, K.; Kiyota, H.; Iwasaki, T.; Nakamura, Y.; Akiba, Y.; Kurosu, T.; Iida, M.; Nakamura, T. *Appl. Phys. A* **1990**, *51*, 334.
10. Veerasamy, V. S.; Amaratunga, G. A. J.; Davis, C. A.; Timbs, A. E.; Milne, W. I.; Mckenzie, D. R. *J. Phys. Condens. Matter* **1993**, *5*, L169.
11. Astier, M.; Pottier, N.; Bourgoin, J. C. *Phys. Rev. B* **1979**, *19*, 5265.
12. Bachelet, G. B.; Baraff, G. A.; Schluter, M. *Phys. Rev. B* **1981**, *24*, 4736.
13. Jackson, K.; Pederson, M. R.; Harrison, J. G. *Phys. Rev. B* **1990**, *41*, 12641.
14. Kajihara, S. A.; Antonelli, A.; Bernholc, J.; Car, R. *Phys. Rev. Lett.* **1991**, *66*, 2010.
15. Kajihara, S. A.; Antonelli, A.; Bernholc, J. *Mater. Res. Soc. Symp. Proc.* **1990**, *162*, 315.
16. Anderson, A. B.; Mehandru, S. P. *Phys. Rev. B* **1993**, *48*, 4423.
17. Giling, L. J.; Wang, Y. S.; Cao, G. Z.; Bauhuis, G. J.; Alkemade, P. F. A. in *Advances in New Diamond Science and Technology*, Sato, S.; Fujimori, N.; Fukunaga, O.; Kamo, M.; Kobashi, K.; Yoshikawa, M. (eds.), Tok-

yo, **1994**, p 359.
18. Shiomi, H.; Tanabe, K.; Nishibayashi, Y.; Fujimori, N. *Jpn. J. Appl. Phys.* **1990**, *29*, 34.
19. Schauer, S. N.; Flemish, J. R.; Wittstruck, R.; Landstrass, M. I.; Plano, M. A. *Appl. Phys. Lett.* **1994**, *64*, 1094.
20. Flemish, J. R.; Schauer, S. N.; Wittstruck, R. Landstrass, M. I.; Plano, M. A. *Diam. Relat. Mater.* **1994**, *3*, 672.
21. Dannefaer, S.; Zhu, W.; Bretagnon, T.; Kerr, D. *Phys. Rev. B* **1996**, *53*, 1979.
22. Hoffmann, R. *J. Chem. Phys.* **1963**, *39*, 1397.
23. Whangbo, M.-H.; Hoffmann, R. *J. Am. Chem. Soc.* **1978**, *100*, 6093.
24. Whangbo, M.-H.; Hoffmann, R.; Woodward, R. B. *Proc. R. Soc. London* A **1979**, *366*, 23.
25. Anderson, A. B.; Grantscharova, E. J.; Angus, J. C. *Phys. Rev. B* **1996**, *54*, 14341.
26. Ammeter, J. H.; Bürgi, H. B.; Thibeault, J. C.; Hoffmann, R. *J. Am. Chem. Soc.* **1978**, *100*, 3686.
27. Hoffmann, R. *Solids and Surfaces: A Chemist's View of Bonding in Extended Structures*; VCH; New York, **1988.**
28. Messmer R. P.; Watkins, G. D. *Phys. Rev. B* **1973**, *7*, 2568.
29. Mainwood, A. *J. Phys. C: Solid State Phys.* **1979**, *12*, 2543.
30. Sahoo, N.; Mishra, K. C.; van Rossum, M.; Dass, T. P. *Hyperfine Interact.* **1987**, *35*, 701.
31. Briddon, P. R.; Heggie, M. I.; Jones, R. in *New Diamond Science and Technology*, Messier, R.; Glass, J. T.; Butler, J. E.; Roy, R. (eds.), Pittsburgh, **1991**, p 63.
32. Erwin, S. C.; Pickett, W. E. *Phys. Rev. B* **1990**, *42*, 11056.
33. Cao, G. Z.; Driessen, F. A. J. M.; Bauhuis, G. J.; Giling, L. J.; Alkemade, P. F. A. *J. Appl. Phys.* **1995**, *78*, 3125.
34. Cao, G. Z.; van Enckevort, W. J. P.; Giling, L. J.; de Kruif, R. C. M. *Appl. Phys. Lett.* **1995**, *66*, 688.
35. Cao, G. Z.; Giling, L. J.; Alkemade, P. F. A. *Diam. Relat. Mater.* **1995**, *4*, 775.
36. Anderson, A. B.; Kostadinov, L. N. *J. Appl. Phys.* **1997**, *81*, 264.
37. Clark, C. D.; Dean, P. J.; Harris, P. V. *Proc. R. Soc.* London A **1964**, *277*, 312.
38. *Tables of Parameters for Extended Hückel Calculations*; collected by Alvarez, S., Universitat de Barcelona, 1993.

Theoretical Study of the Reactions of H+H_2 and Its Isotopic Variants Inter- and Intramolecular Isotope Effect

Ju-Beom Song

Department of Chemical Education, Kyungpook National University, 1370 Sankyuk-Dong, Pook-Ku, Taegu 702-701, Korea
Received January 11, 1998

Quasiclassical trajectory calculations were carried out for the reactions of H+H_2 (v=0, J=0) and its isotope variants on the Siegbahn-Liu-Truhlar-Horowitz potential energy surface for the relative energies E between 6 and 150 kcal/mol. The goal of the work was to understand the inter- and intramolecular isotope effects. We examine the relative motion of reactants during the collision using the method of analysis that monitors the intermolecular properties (internuclear distances, geometry of reactants, and final product). As in other works, we find that the heavier the incoming atom is, the greater the reaction cross section is at the same collision energy. Using the method of analysis we prove that the intermolecular isotope effect is contributed mainly by differences in reorientation due to the different reduced masses. We show that above E=30 kcal/mol recrossing also contributes to the intermolecular isotope effect. For the intramolecular isotope effect in the reactions of H+HD and T+HD, we reach the same conclusions as in the systems of O(^{3}P)+HD, F+HD, and Cl+HD. That is, the intramolecular isotope effect below E=150 kcal/mol is contributed by reorientation, recrossing, and knockout type reactions.

Introduction

Recently, we have carried out a series of quasiclassical trajectory (QCT) computations[1-10] for gas phase exchange reactions such as

$$X+H_2 \rightarrow XH+H, \quad (1)$$
$$X+HD \rightarrow XH+D, \quad (2a)$$
$$\rightarrow XD+H, \quad (2b)$$

where X is O(^{3}P), F, Cl, T, and H, in order to understand the effect of translational, vibrational, and rotational energy in the reactants on the reactive cross section. For all of the systems we have studied there is a barrier to reaction which is lowest in the linear configuration and which grows as the X-H-H angle is bent. We have also examined the inter- and intramolecular isotope effects in some of these reactions. In the QCT works certain intermolecular properties (bond